Knowledge Gained From Instrumentation of the Kishwaukee River Bridge

K. Nam Shiu
Structural Engineer
Structural Experimental Section
Construction Technology Laboratories
Portland Cement Association
Skokie, Illinois

Henry G. Russell
Director
Structural Development Department
Construction Technology Laboratories
Portland Cement Association
Skokie, Illinois

The Kishwaukee River Bridge, shown in Fig. 1, consists of two long span post-tensioned concrete segmental box girder bridges. The bridges, made of precast segments, were erected by the balanced cantilever method of construction using a launching truss system.[1] This application of the launching truss for bridge erection was the first in the United States.[2]

In the balanced cantilever method of construction, bridge segments undergo different stress conditions during and after construction. Therefore, the bridge design has to include every construction event that results in significant stress changes. In addition, the time-dependent effects of creep, shrinkage, and temperature must be taken into account.

Verification of design assumptions using measured data is needed and is essential to the successful prediction of long-term bridge deformations. Therefore, an investigation to obtain field data on an existing bridge was made to verify analytical and design procedures for predicting time-dependent behavior of post-tensioned box girder bridges.

The investigation comprised three parts:

1. Field measurements on Kishwaukee River Bridge.
2. Laboratory measurements of concrete used in the bridge.
3. Comparisons between field measurements and calculated deformations.

Field measurements included longitudinal concrete strains, vertical deflections, and temperatures of three bridge segments. Initial readings were taken as soon as possible after placement of concrete. Readings presented a detailed record of bridge behavior over a period of 5 years.

Fig. 1. Kishwaukee River Bridge.

Synopsis

The objectives of the instrumentation program were to measure and evaluate the behavior of a long span box girder bridge. Three bridge segments were instrumented. Field measurements were taken from the beginning of bridge construction for a total period of 5 years. Properties of concrete used in the instrumented segments were determined in the laboratory.

Using the measured concrete properties and detailed construction records, time-dependent deformations of the bridge segments were calculated by a step-by-step numerical procedure. Calculated deformations were compared with measured data to verify the numerical procedure. Subsequently, the numerical procedure was used to determine information that could not be obtained by field measurements. Findings with regard to axial deformations, prestress losses, moment redistribution, concrete stresses, and temperature effects are presented.

Laboratory tests were made to determine the properties of concrete used in the bridge. Measured concrete properties included variation of compressive strength, modulus of elasticity, Poisson's ratio, and coefficient of thermal expansion with time. Measured time-dependent properties were creep and shrinkage of concrete. Information obtained from laboratory measurements was used in the analytical studies.

A computer program using a step-by-step numerical procedure to determine time-dependent behavior of box girders was used. The computer program was developed at the University of Illinois at Urbana by Marshall and Gamble.[3] The actual construction schedule was used in the analyses. Comparisons between field measurements and calculated results verified the numerical procedure. The numerical procedure was then used to determine information that could not be obtained from field measurements.

FINDINGS

The following findings were obtained from the evaluation of time-dependent deformations on the Kishwaukee River Bridge:

1. Longitudinal deformations calculated by a step-by-step numerical procedure were in good agreement with measured values.

2. Based on temperature measurements taken on four randomly selected days, the maximum measured variation of air temperature between seasons was 60 F (33 C). Within a 24-hour period, a maximum temperature difference of 25 F (14 C) was measured.

3. Measured temperature distributions across sections of the bridge were nonlinear. Temperature distribution profiles varied with fluctuations of air temperatures inside and outside the box girder.

4. Maximum measured temperature differentials between the top slab and bottom slab were 15 F (8 C) and −20 F (−11 C).

5. Calculated prestress losses caused by concrete creep and shrinkage during the first 1850 days after erection were less than values determined by AASHTO Specifications.[4]

6. Calculated prestress losses caused by relaxation of post-tensioning tendons were greater than values recommended by AASHTO Specifications.[4]

7. Five years after bridge completion, redistributed moments from concrete creep were calculated to be 14 percent of support moments and 56 percent of midspan moments. However, redistribution of moments is unlikely to result in flexural tensile stresses in the superstructure.

8. Compressive concrete stresses at the top and bottom of each instrumented segment tended to equalize as a result of time-dependent deformations.

RECOMMENDATIONS

1. Time-dependent behavior analysis of post-tensioned segmental concrete bridges should be based on actual concrete material properties. Best prediction of time-dependent behavior is obtained when data for concrete stored outdoors are used. However, good agreement is obtained when data for concrete cured indoors are used.

2. Based on measured temperature differentials between the top slab and bottom slab of the bridge, a design temperature differential of −9 F (−5 C) may not be sufficient for midwestern states. A maximum temperature differential of −20 F (−11 C) was recorded during four randomly selected days of measurements.

3. Calculated prestress losses due to concrete creep and shrinkage were less than those calculated using AASHTO Specifications[4] which do not take into
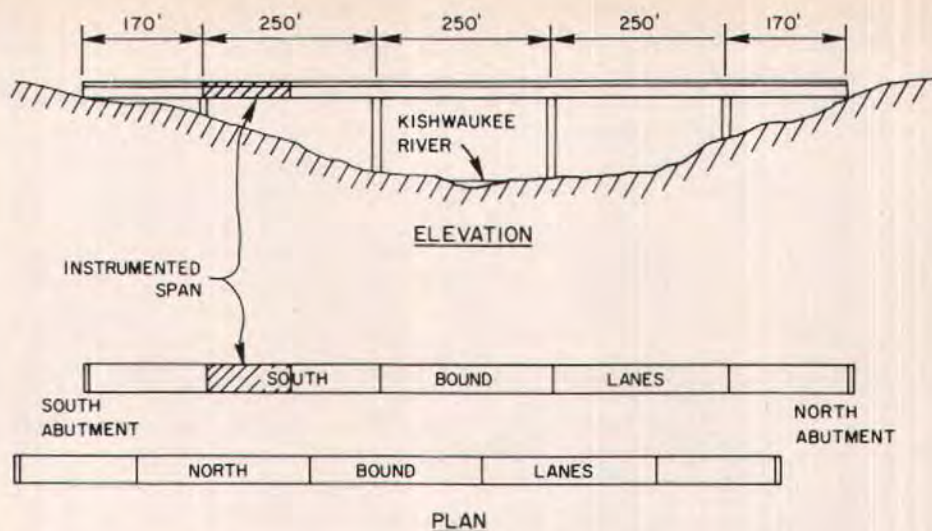
Fig. 2. Elevation and plan of Kishwaukee River Bridge (Note: 1 ft = 0.305 m).

account concrete age at erection and member thickness. Further investigation of creep and shrinkage effects on prestress losses is recommended.

4. Estimation of prestress losses for the relaxation of post-tensioning tendons according to AASHTO Specifications[4] should be further investigated. Current specifications seem to underestimate prestress losses due to relaxation in post-tensioning tendons.

5. Moment redistribution due to time-dependent effects should be accounted for in design of long span continuous bridges. An increase of positive moments by as much as 56 percent at midspan was predicted in the analysis of the Kishwaukee River Bridge.

FIELD MEASUREMENTS

The Kishwaukee River Bridge[5] consists of two identical continuous single cell box girders made with precast concrete segments. Each girder has three main spans of 250 ft (76.2 m) and two approach spans of 170 ft (51.8 m) for a total length of 1090 ft (332 m). Eleva-

tion and plan views of the bridge are shown in Fig. 2.

Each span was constructed by cantilevering segments out from both sides of the main pier. A 150-ton (136 t) launching truss was used to facilitate positioning and erection of each segment. Fig. 3 shows the positioning of a bridge segment before temporary post-tensioning. At the completion of construction, spans were made continuous for live loads.

Each main span consisted of 34 precast segments with one cast-in-place closure segment at midspan. Longitudinal post-tensioning was provided in the top and bottom slab of the box section. The top slab was also prestressed transversely. Straight threaded 1¼-in. (32 mm) diameter bars were used as longitudinal tendons. Other details of construction have been reported previously.[1]

Three segments in one 250-ft (76.2 m) span of the south bound lane bridge were selected for instrumentation as shown in Fig. 2. Locations of the selected segments are identified in Fig. 4

as SB1-N1, SB1-N9, and SB1-N16. These segments were located next to the pier support, at quarter span, and near midspan. A detailed description of the field instrumentation is given elsewhere.[5]

Field measurements included readings of longitudinal concrete strains, vertical deflections, air temperatures, and concrete surface temperatures.

Fig. 3. Launching truss facilitates erection and positioning of bridge segment prior to temporary post-tensioning.

Longitudinal Strains

Longitudinal strains were measured in three instrumented segments. Locations of strain measurements are shown in Fig. 5. Measurements were made with a Whittemore mechanical strain gage and 24 Carlson strain meters. The Whittemore strain gage measured longitudinal surface deformations between fixed reference points. Reference points were glued to the inside concrete surface of the box segment soon after steam curing.

The Carlson strain meters measured internal concrete strains and temperatures. Meters were installed by tying to the reinforcement cage, shown in Fig. 6, before casting. All Carlson meters were embedded in concrete. To have a detailed account of the bridge behavior, longitudinal strain readings were taken before and after every known significant event that changed the strain histories of bridge segments.

The strain history of Segment SB1-N1 is shown in Fig. 7. It is noted that the large increase in compressive strain at about 100 days corresponds to erection of the bridge segment. A similar longitudinal strain history pattern was observed in the other two instrumented segments.

It is also noted that seasonal strain variations of about 50 millionths can be observed in Fig. 7 even though all recorded strains had been corrected for temperature to 73 F (23 C). The correc-
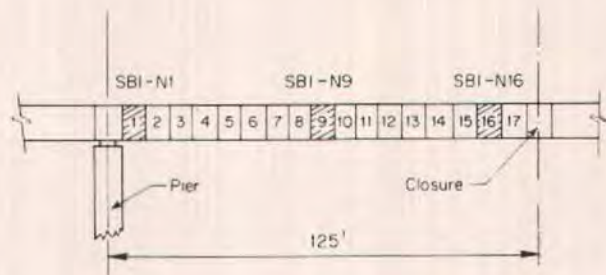

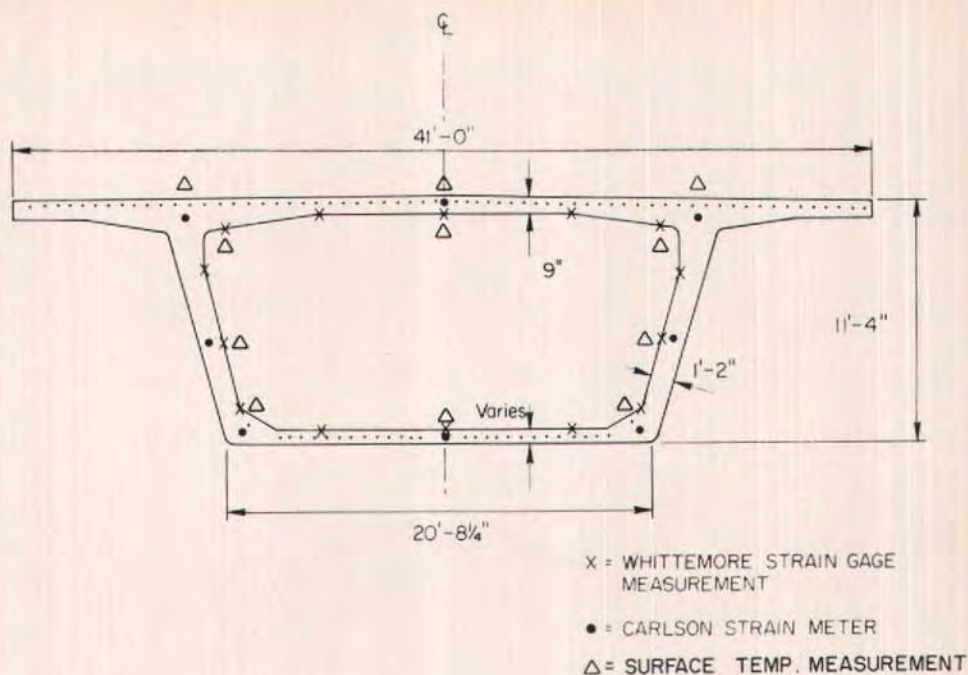Fig. 4. Locations of instrumented segments (Note: 1 ft = 0.305 m).

Fig. 5. Locations of longitudinal strain measurements in bridge segment.
Measurements were made with a Whittemore mechanical strain gage and 24 Carlson
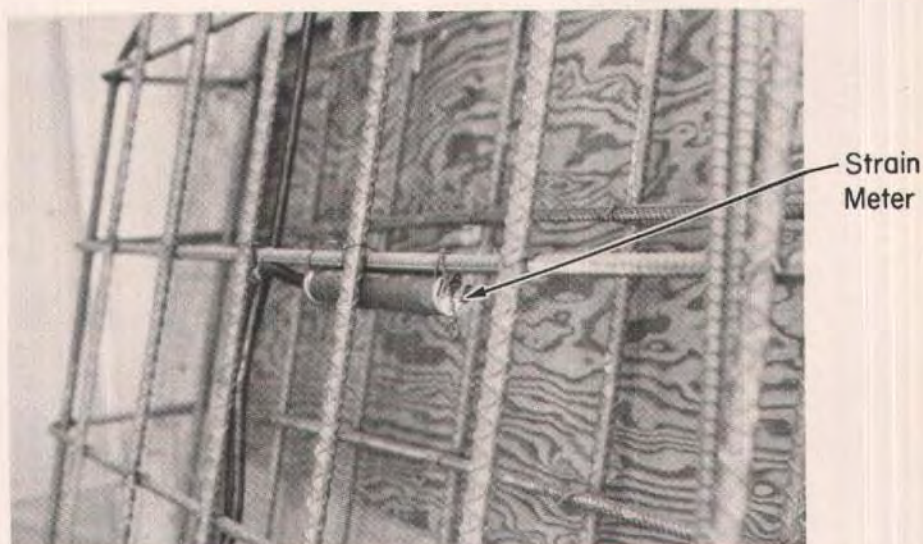strain meters (Note: 1 ft = 0.305 m).

Fig. 6. Installation of Carlson strain meter by tying to reinforcement cage. Meters were
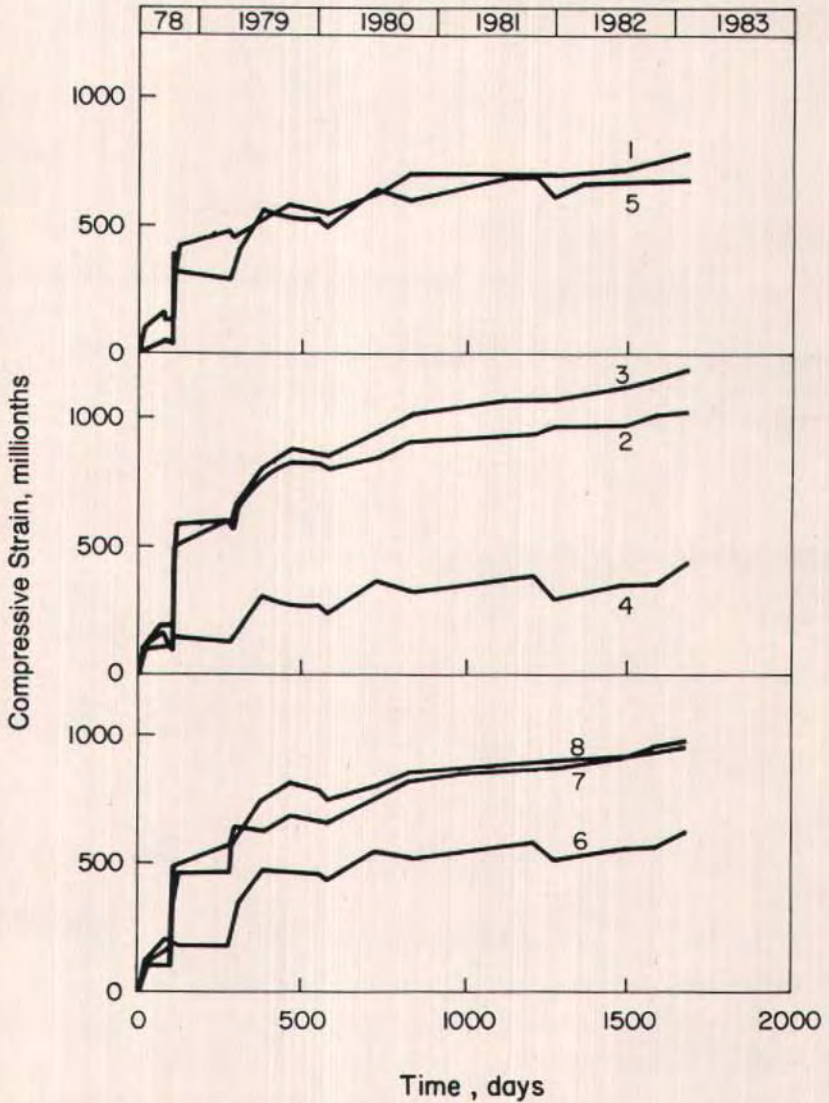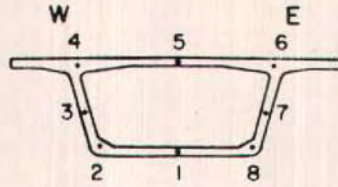subsequently embedded in concrete.

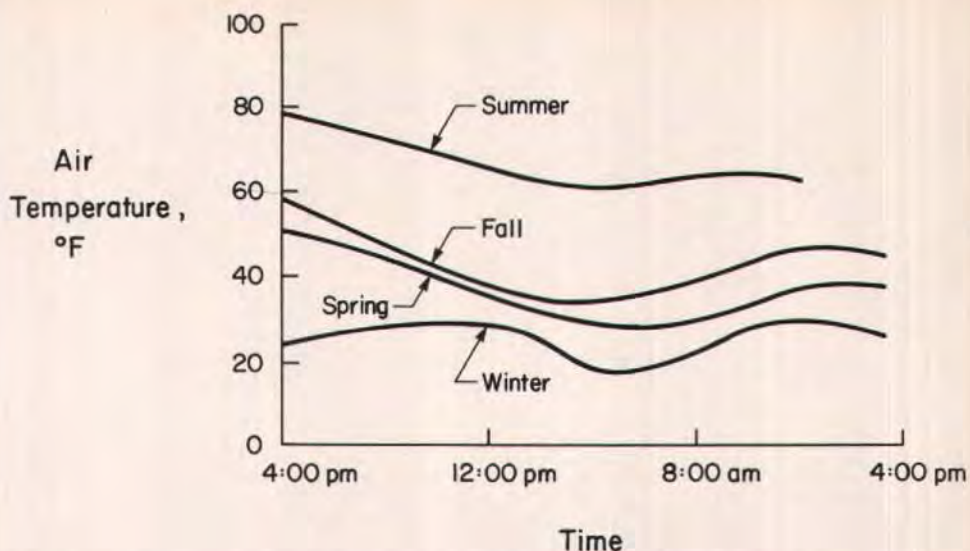Fig. 7. Carlson strain data for Segment SB1-N1.

Fig. 8. Air temperature variation over 24 hours for different seasons (Note: 1°F = 0.56°C).

tion was based on the assumption that concrete and strain gages expand and contract freely according to the linear coefficient of thermal expansion. The seasonal strain fluctuation was especially obvious for longitudinal strains measured in the top slab of the box girder. This phenomenon was attributed to effects of varying outdoor temperatures and relative humidities at the bridge site.

Both Carlson strain meter readings and the Whittemore gage readings yielded consistent and similar results. In this paper, only data from the Carlson strain meters are discussed.

Temperature

Temperature measurements included air temperatures, concrete surface temperatures, and internal concrete temperatures. Air temperatures were measured by a thermometer. Readings included air temperature inside and outside the box section. Surface temperatures were measured by a portable surface thermocouple. Internal concrete

temperatures were calculated from Carlson strain readings. Locations of temperature measurements are given in Fig. 5. From temperature measurements, temperature gradients through the top slab of the box section were obtained. Relative humidities inside and outside the box girder were also recorded.

In addition to regular field measurements, temperature readings were taken in four 24-hour periods. Each 24-hour period represented one season. Variations of measured air temperatures at the bridge over the four 24-hour periods are plotted in Fig. 8. From the collected data, the maximum seasonal temperature variation of 60 F (33 C) was observed. Within a 24-hour period, the maximum recorded temperature difference was 25 F (14 C).

Measured temperature distributions across bridge sections were nonlinear. Temperature profiles of the bridge in summer and winter of 1979 are shown in Fig. 9. Maximum measured temperature differentials between the top slab and bottom slab were 15 F (8 C) and
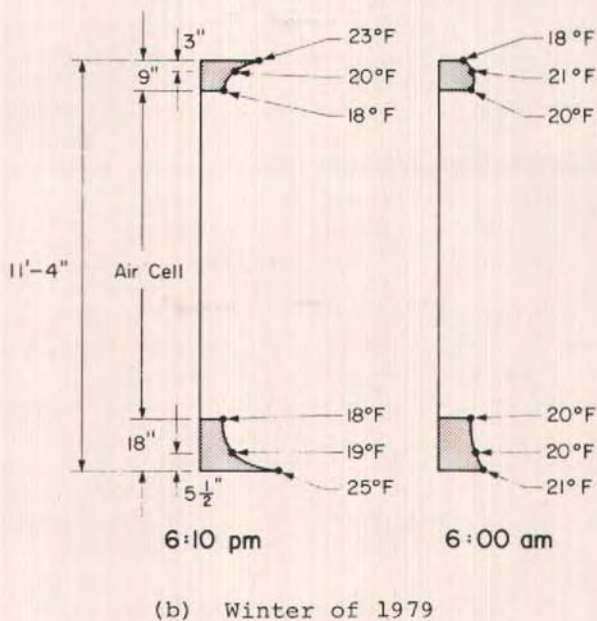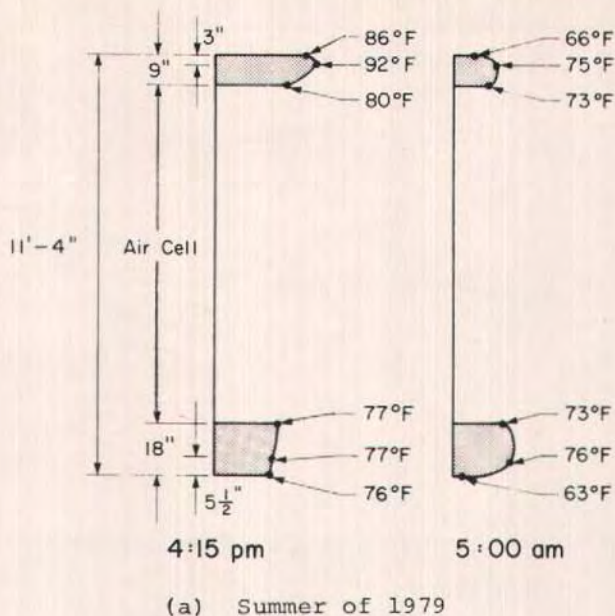
(a) Summer of 1979

(b) Winter of 1979

Fig. 9. Temperature distribution across Segment SB1-N1
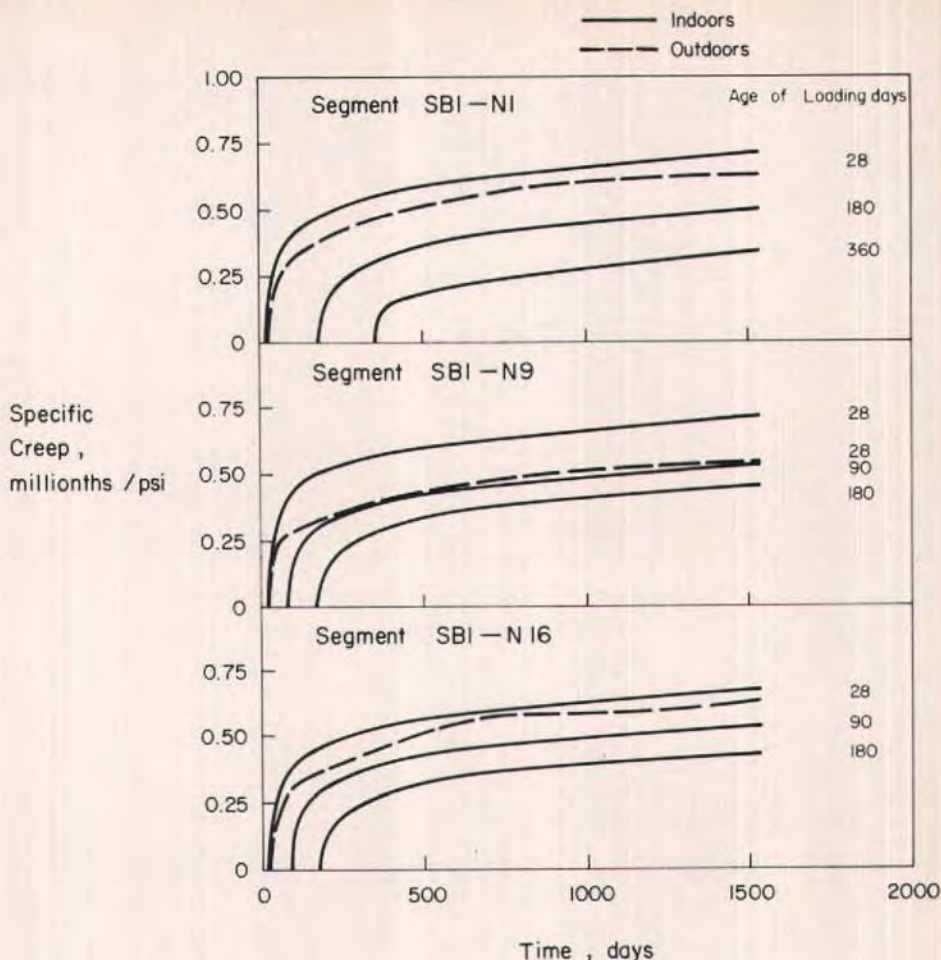(Note: 1 ft = 0.305 m; 1°F = 0.56°C).

Fig. 10. Specific creep versus time (Note: 1 millionth/psi = 145 millionths/N/mm²).

−20F (−11 C). The design differentials were 18 F (10 C) and −9 F (−5 C). Thus, the negative measured temperature differential was larger than the design value.

LABORATORY MEASUREMENTS

Properties of concrete used in the instrumented segments were determined. Tests were performed on concrete cylinders made at the precasting plant where bridge segments were cast. The

tests determined variations of concrete compressive strength, modulus of elasticity, Poisson's ratio, and coefficient of thermal expansion of concrete with time.

Creep tests for concrete cylinders under constant temperature of 73 F (23 C) and 50 percent relative humidity were initiated at three different ages. Tests were conducted conforming to ASTM Designation: C512-82.[6] All creep cylinders were subjected to a constant stress of 2000 psi (13.8 MPa). Whenever creep measurements were made, com-
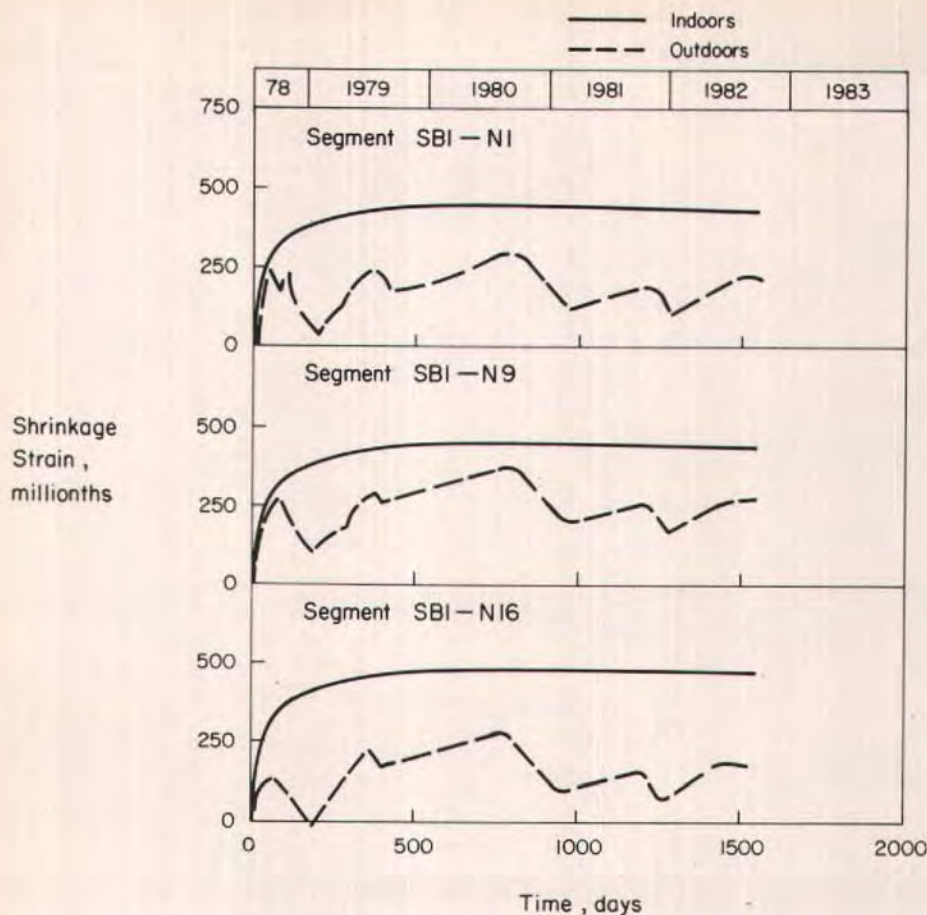
Fig. 11. Shrinkage strain of concrete versus time.

panion shrinkage measurements were also obtained.

Similar creep tests for cylinders cured under an outdoor environment were started at concrete age of 28 days. In addition to regular creep readings, measurements on outdoor creep cylinders were made once every season. Measurements were needed to evaluate effects of seasons on time-dependent concrete properties.

Variation of concrete specific creep with time for each instrumented segment is shown in Fig. 10. Specific creep is defined as the amount of creep strain under unit stress in millionths

per psi (millionths/N/mm²). Concrete shrinkage was excluded from specific creep readings. Solid curves in Fig. 10 represent specific creep of concrete loaded at different concrete ages. The dashed lines represent relationships of specific creep versus time for concrete cured outdoors. All readings were adjusted for temperature effects to 73 F (23 C) for comparison purposes.

As shown in Fig. 10, relationships of specific creep versus time for concretes loaded at the same age were similar. In addition, specific creep was lower for concrete cured outdoors than for concrete cured indoors.

Shrinkage measurements of concrete cylinders began 7 days after casting. A comparison of shrinkage data for specimens cured indoors and those cured outdoors is shown in Fig. 11. The solid line in Fig. 11 represents shrinkage of concrete cured under laboratory conditions. The dashed line in the figure indicates shrinkage of concrete cured outdoors. Fig. 11 shows that shrinkage of concrete cured outdoors was substantially less than concrete cured indoors. In addition, there was a distinct seasonal fluctuation of concrete shrinkage under outdoor conditions.

COMPUTER ANALYSIS

Time-dependent deformations were calculated by a step-by-step numerical procedure. Total shortening was considered to include instantaneous deformation, shrinkage deformation, and creep deformation. Analyses accounted for time-dependent effects of concrete properties, relaxation of prestressing steel, member thicknesses, elastic recovery, age of loading, shrinkage, and creep of concrete under a variable stress history. The actual casting and erection schedule of bridge segments was used. Further details of the numerical procedure are given elsewhere.[3]

Analyses were performed for three different sets of material properties. In Analysis No. 1, experimentally determined properties of concrete specimens stored outdoors were used. In Analysis No. 2, concrete properties determined from specimens cured indoors were used. For Analysis No. 3, material properties recommended by the European Concrete Committee[7] were used.

COMPARISON OF MEASURED AND CALCULATED STRAINS

Measured and calculated results were compared with regard to longitudinal concrete strains. Comparisons verified the numerical procedure.

Comparisons between measured and calculated strains from the three analyses of Segment SB1-N1 are shown in Fig. 12. Detailed comparisons are presented elsewhere.[3,5] The best agreement was obtained with Analysis No. 1 which used concrete properties of cylinders stored outdoors. Good comparison was obtained with Analysis No. 2 using properties of laboratory cured concrete cylinders. In Analysis No. 3, calculated strains were consistently smaller than measured values.

Comparisons of measured and calculated strains using Analysis No. 1 for Segments SB1-N9 and SB1-N16 are shown in Fig. 13. Good agreement between measured and calculated strains was obtained. Comparisons between measured and calculated strains for Segments SB1-N9 and SB1-N16 using Analysis No. 2 also showed good agreement. These comparisons show that the numerical procedure was able to predict deformations reasonably close to measured deformations. Consequently, the numerical procedure was used to determine information that could not be obtained directly by field measurements.

SIGNIFICANCE OF RESULTS

Discussions of results with regard to axial deformations, prestress losses, moment redistribution, concrete stresses, and temperature effects are presented.

Axial Deformations

Comparisons of measured and calculated axial strains for the three instrumented segments of the bridge are shown in Figs. 12 and 13. Calculated deformations for Segment SB1-N1 at 2000 days since erection were 380 mil-
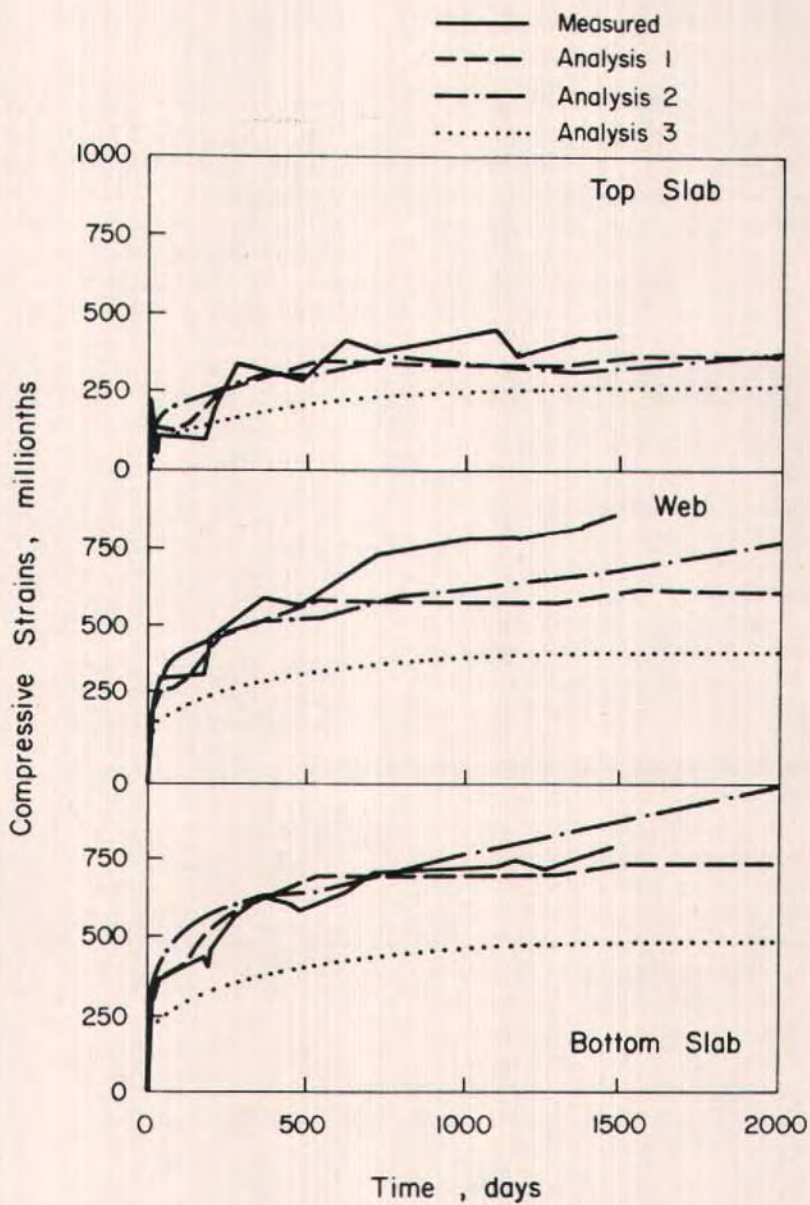
Fig. 12. Comparison of measured and calculated strains for Segment SB1-N1.
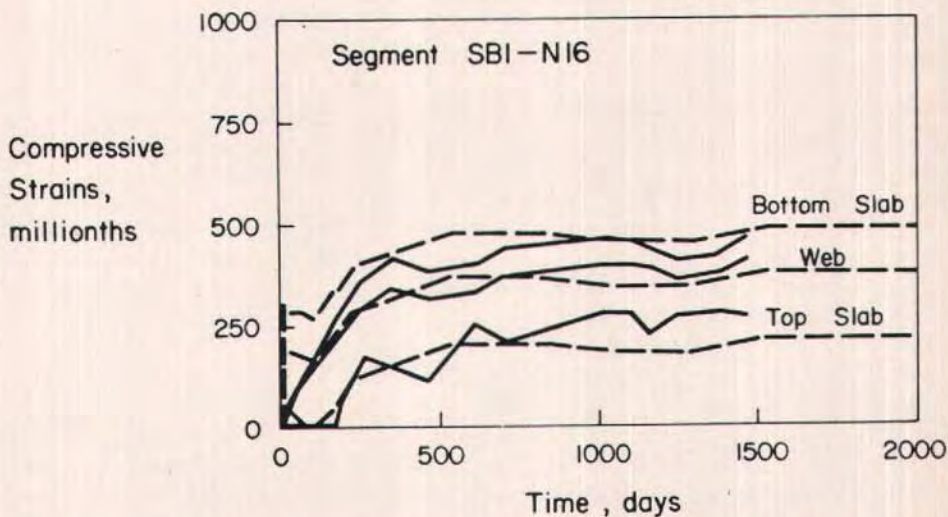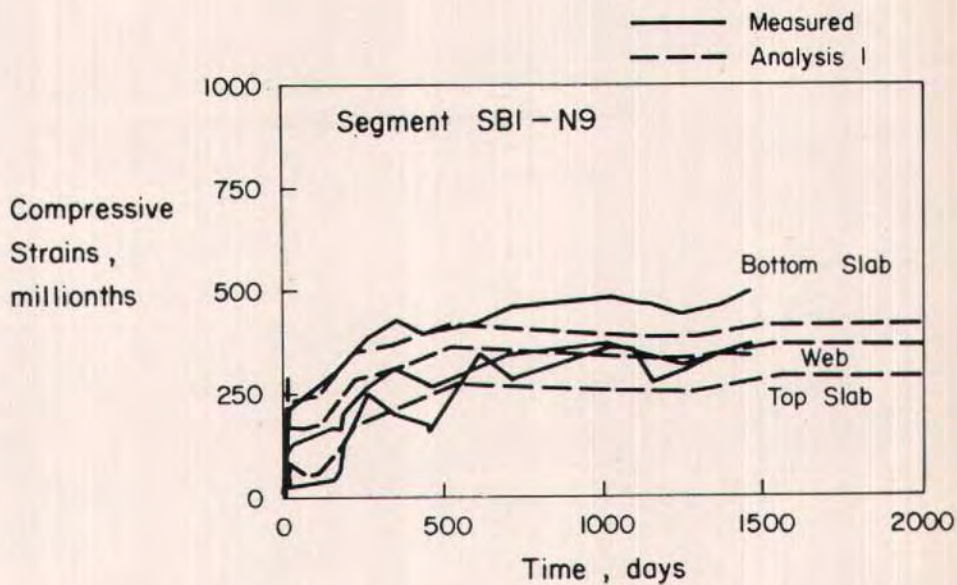
Fig. 13. Comparison of measured and calculated strains for Segments SB1-N9 and SB1-N16.
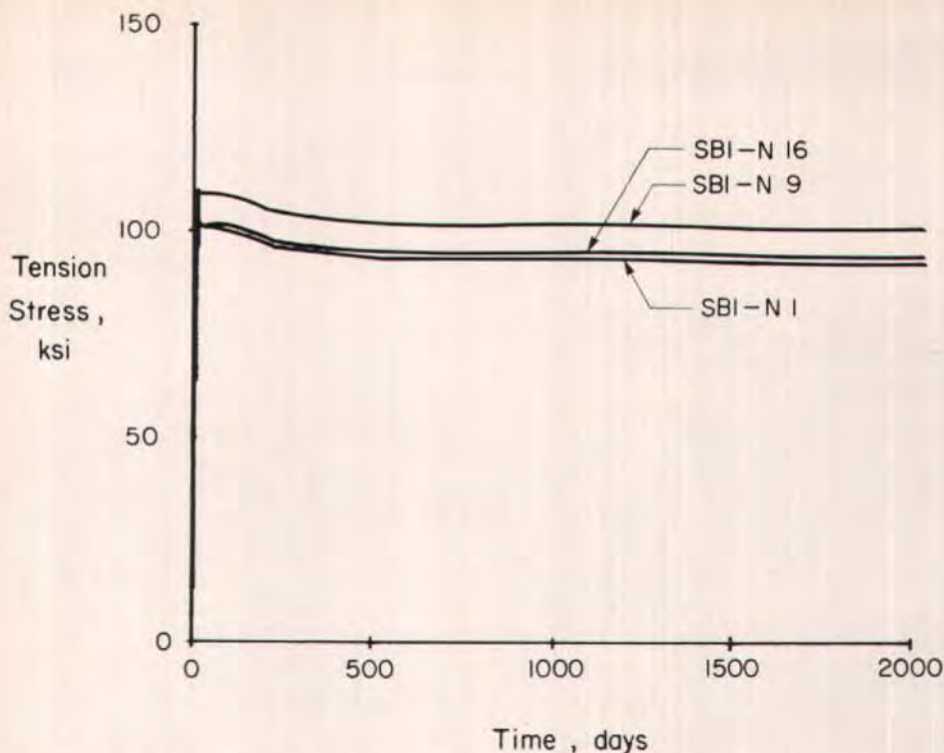
Fig. 14. Calculated average tendon stresses (Note: 1 ksi = 6.89 MPa).

lionths in the top slab and 780 millionths in the bottom slab. An axial deformation of 780 millionths represents a shortening of 2.3 in. (59 mm) in a 250-ft (76.2 m) span. In Segment SB1-N16, axial strains of 197 and 486 millionths were calculated for the top and bottom of the box section, respectively.

However, the majority of the axial deformation occurred during construction of the cantilever spans. Calculated axial deformations for Segment SB1-N1 after completion of construction ranged from 143 to 233 millionths at 2000 days since erection. This accounts for 30 to 40 percent of the total measured shortening. Consequently, most of the deformation was accommodated when the closure segment was cast at midspan. Therefore, only shortening that occurred after completion of the bridge

need be considered in determining overall longitudinal movements.

Prestress Losses

The numerical procedure was used to determine variation of prestressing force with time. Calculated changes of prestressing force with time for the three instrumented segments are shown in Fig. 14. Calculated values are based on Analysis No. 1 which used material properties of concrete cured outdoors. Tendon stresses are the average values for tendons in each instrumented segment. It is noted that total prestress losses are relatively small and are approximately equal for each segment.

Individual prestress losses caused by time-dependent effects as predicted by Analysis No. 1 are summarized in Table

Table 1. Summary of prestress losses for Segments SB1-N1, SB1-N9, and SB1-N16.

| Segment | Prestress losses (psi) | | | | | |
| | Shrinkage | | Creep | | Relaxation | |
	Analysis	AASHTO	Analysis	AASHTO	Analysis	AASHTO
SB1-N1	879*	4840	5460	6360	3620	3000
SB1-N9	880*	4840	5430	6660	4020	3000
SB1-N16	585*	4840	6820	9340	3750	3000

Metric Equivalent: 1 psi = 6.89 Pa.

*Values represent maximum prestress losses from concrete shrinkage calculated for the second year after segment erection.

1. For comparison, prestress losses calculated according to AASHTO Specifications[4] are also listed. It is noted that analytical values shown in Table 1 represent prestress losses at approximately 1850 days after the segments were erected.

Table 1 shows that calculated losses from creep and shrinkage are less than those calculated according to AASHTO Specifications.[4] Differences between calculated and AASHTO specified values are especially large for prestress losses due to concrete shrinkage. The reason for the small calculated prestress losses was that concrete under outdoor conditions experienced less creep and shrinkage as shown in Figs. 10 and 11.

In addition, concrete cured outdoors exhibited seasonal shrinkage variations which were also reflected in the calculated prestress losses. Therefore, AASHTO Specifications overestimated prestress losses due to concrete creep and shrinkage. However, calculated relaxation losses were slightly larger than the 3000 psi (21 MPa) given in AASHTO Specifications.[4]

It should be also noted that the instrumented segments were erected at approximately 100 days after casting. However, AASHTO Specifications[4] do not consider ages of concrete segments at time of erection. Furthermore, the Specifications do not take into account

member thickness. Therefore, differences between prestress losses according to AASHTO Specifications[4] and the calculated values are expected.

Moment Redistribution

As a result of time-dependent deformations, redistribution of bending moments takes place in a continuous structure. Using Analysis No. 1, time-dependent redistribution of moments in the Kishwaukee River Bridge was calculated. Distribution of bending moment at the time of bridge completion and at 1850 days after completion are shown in Fig. 15.

The general redistribution trend was to shift moment from negative moment regions to positive moment regions. The magnitudes of positive bending moments increased with time while magnitudes of negative bending moments decreased with time. The positive increase of bending moment throughout each span was found to be similar. However, the percentage of moment change at the pier and at midspan varied significantly. Due to the relatively high initial negative moments, a small percentage decrease in negative moment corresponded to a large percentage increase in positive moment. Calculated results indicated an average 14 percent decrease in moment at the pier and an average 56 per-
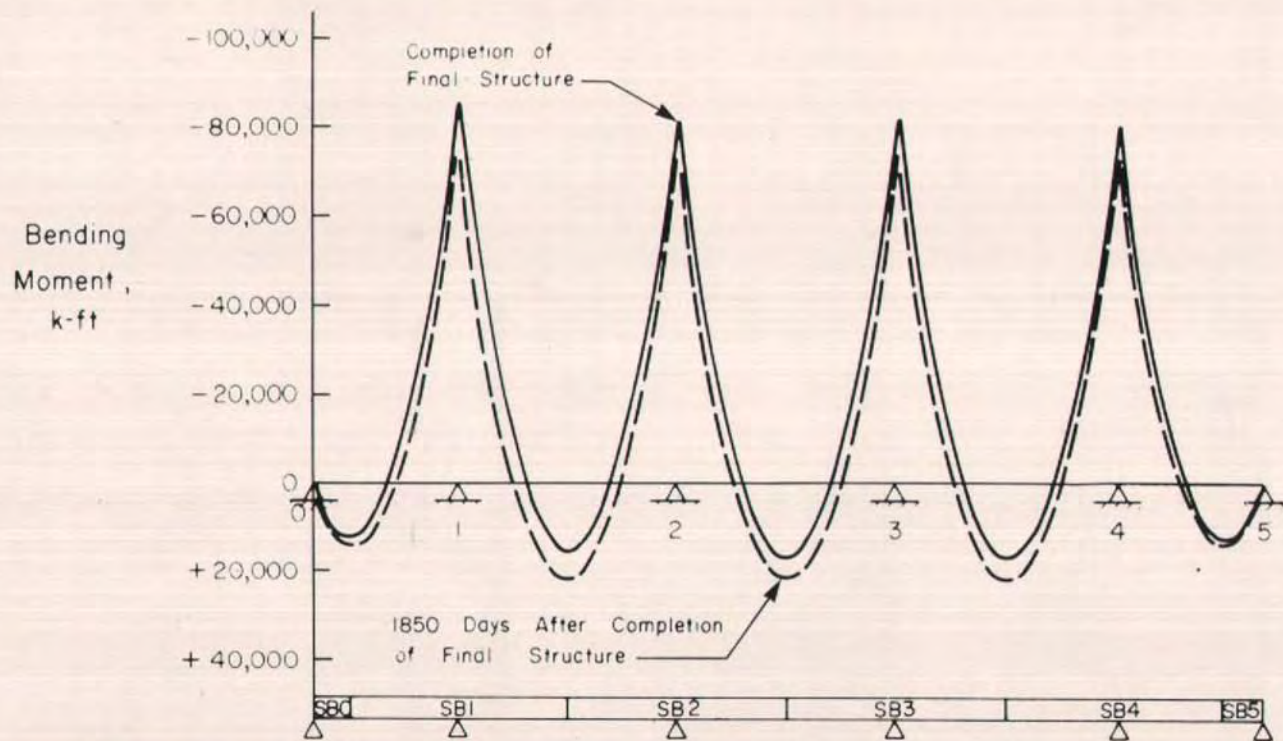
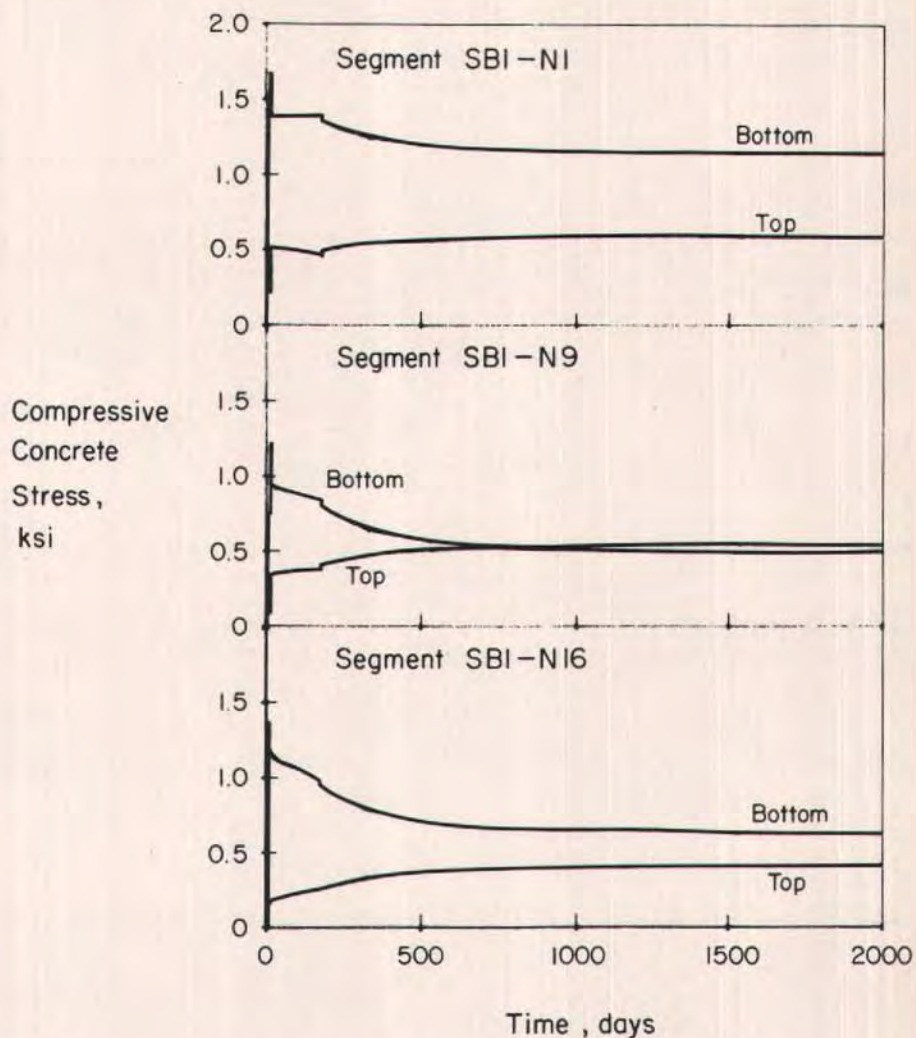Fig. 15. Redistribution of bending moments (Note: 1 k-ft = 1.35 kN-m).

Fig. 16. Calculated concrete stresses from Analysis No. 1 (Note: 1 ksi = 6.89 MPa).

cent increase of midspan moment between piers.

The large increase in positive moments is especially significant at the quarter span where the direction of bending moment may change as a result of redistribution. Therefore, designs must account for time-dependent increase in positive moments.

Concrete Stresses

As indicated from Analysis No. 1, there was a large increase of positive moment at midspan of the bridge. However, the calculated concrete stresses from Analysis No. 1 indicated no danger of cracking as a result of moment redistribution. Calculated
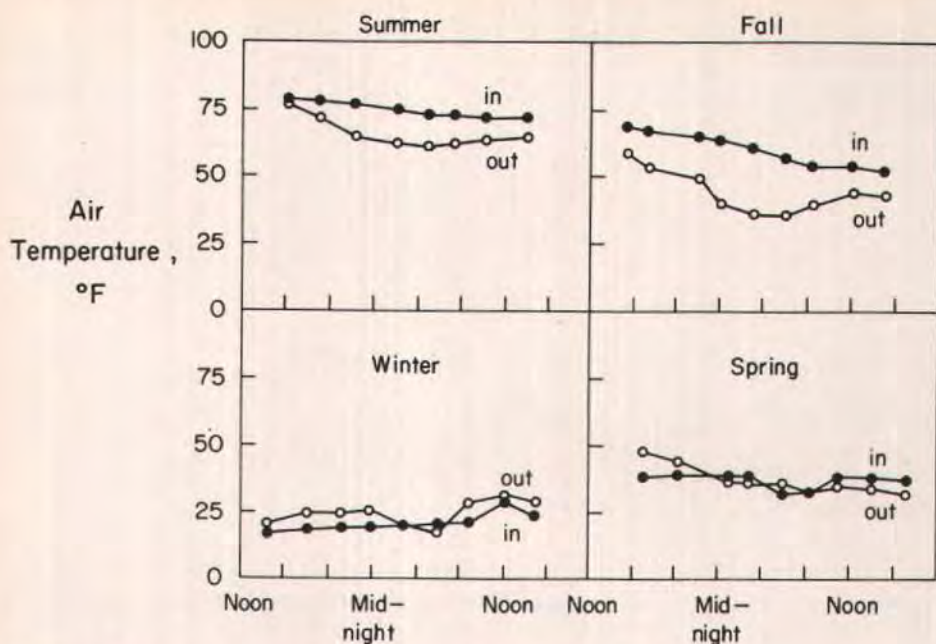
Fig. 17. Daily variations of air temperatures inside and outside the box girder in four seasons (Note: 1°F = 0.56°C).

stresses by Analysis No. 1 for each of the instrumented segments are shown in Fig. 16.

In general, compressive stresses in the top slabs increased with time while compressive stresses in the bottom slabs decreased with time. These data are consistent with the redistribution of moment occurring throughout the bridge. In Fig. 16, there is a substantial decrease in compressive stress at the bottom slab of Segment SB1-N16. However, the stress reduction was not sufficient to cause concern about cracking at midspan. The calculated compressive stress at the bottom of Segment SB1-N16 at 1850 days after erection was approximately 620 psi (4272 Pa).

It should be noted that the stresses are calculated based on actual dead loads of the bridge rather than design service loads. Consequently, stresses resulting from additional dead load or

live load will be additive to values shown in Fig. 16.

Temperature Effects

Variations of air temperatures inside and outside the box girder over 24 hours in four randomly selected days are shown in Fig. 17. Air temperatures inside the box girder were more stable and exhibited less variation than the outside air temperatures. In addition, a time lag was observed in the response of the inside air temperature to the outside environment changes. Consequently, big temperature differentials across the top and bottom slabs and through the webs can exist when there is a sudden change of outside air temperature.

Thermal response of structures to temperature can either be in the form of induced stresses or induced deformations. Therefore, longitudinal strains of
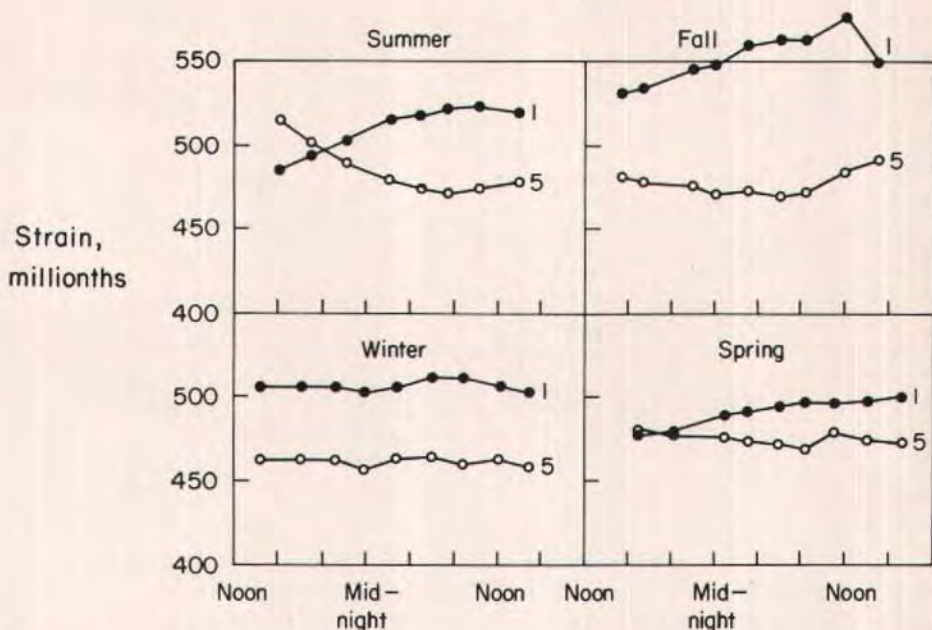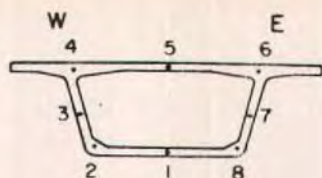
Fig. 18. Daily variations of longitudinal concrete strains of Segment SB1-N1 in four seasons.

the instrumented segments were recorded together with temperature measurements. Figs. 18 through 20 show the variation of concrete strains within a day for the four seasons for Segments SB1-N1, SB1-N9, and SB1-N16, respectively. The strain data have been corrected for temperature of concrete on the basis that the bridge responds freely to temperature change.

Data in Figs. 18 to 20 show comparatively large changes in strain for Segment SB1-N1 due to temperature as compared with responses recorded in Segments SB1-N9 and SB1-N16. Large strain changes due to temperature indicated that the bridge segment re-

sponded in the form of thermal movements. Comparison between measured deformations of the three segments indicated that both thermal stresses and deformations were induced in the bridge. Such thermal stresses should be included in design.
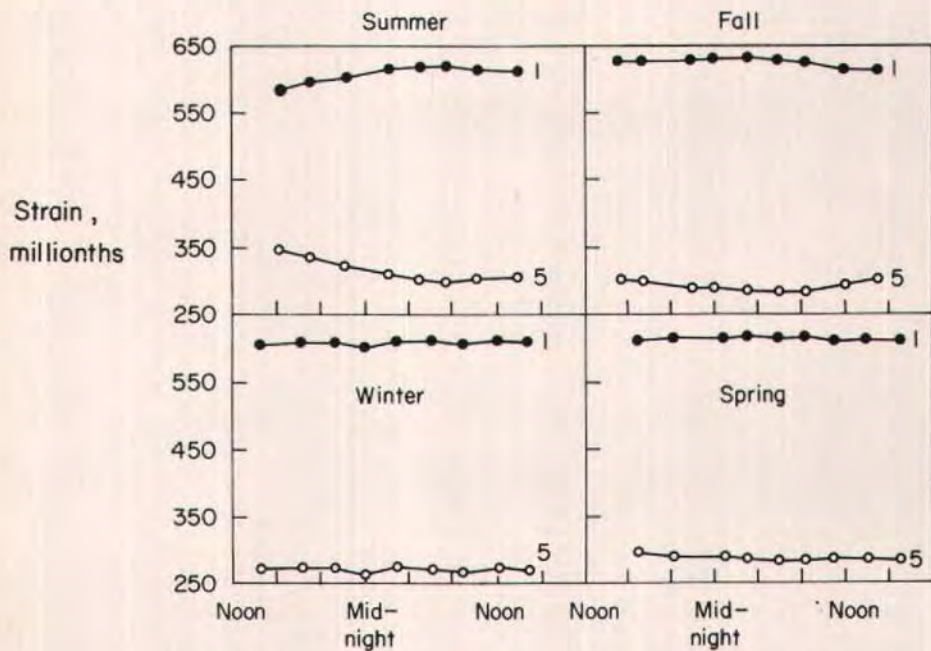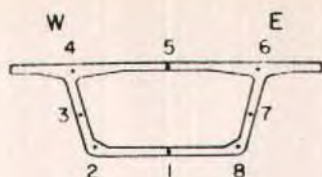
ACKNOWLEDGMENTS

Fig. 19. Daily variations of longitudinal concrete strains of Segment SB1-N9 in four seasons.

Technology Laboratories. James I. Daniel, structural engineer, and Thomas L. Weinmann, project assistant of the Structural Experimental Section, helped in all tests. Their efforts are sincerely appreciated and acknowledged.

Dr. W. L. Gamble and Dr. V. L. Marshall were responsible for the analytical studies. The analytical work was performed at the University of Illinois under an agreement with the Construction Technology Laboratories.

Richard Taylor of the State of Illinois Department of Transportation coordinated the project. Members of the Advisory Committee who reviewed prog-

ress of the project were Robert Appleman, Gayle Lane, Frank Grabski, Donald R. Schwartz, Colin Strang, Richard Taylor, and John Ross. Their contributions to the project are appreciated.

REFERENCES

1. Nair, R. S., and Iverson, J. K., "Design and Construction of the Kishwaukee River Bridges," PCI JOURNAL, V. 27, No. 6, November-December 1982, pp. 22-47.
2. "Truss Launches Quickly in U.S. Box Girder Debut," Engineering News Record, October 19, 1978, pp. 45-58.
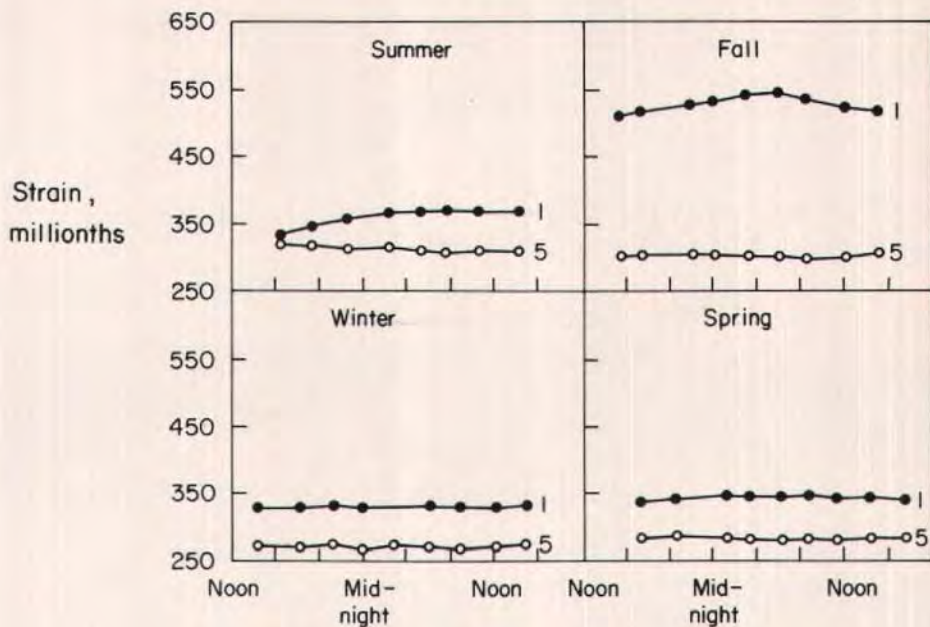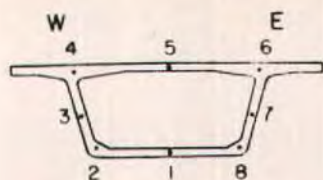
Fig. 20. Daily variations of longitudinal concrete strains of Segment SB1-N16 in four seasons.

3. Marshall, V., and Gamble, W. L., "Time-Dependent Deformations in Segmental Prestressed Concrete Bridges," Structural Research Series No. 495, Civil Engineering Studies, University of Illinois, Urbana, October 1981, 242 pp.

4. *Standard Specifications for Highway Bridges*, Twelfth Edition, American Association of State Highway and Transportation Officials, 1977.

5. Shiu, K. N., Daniel, J. I., and Russell, H. G., "Time-Dependent Behavior of Segmental Cantilever Concrete Bridges," Final Report to the State of Illinois, Department of Transportation, by Construc-

tion Technology Laboratories, a Division of the Portland Cement Association, Skokie, Illinois, March 1983; to be published through National Technical Information Services, Springfield, Virginia.

6. "Standard Method of Test for Creep of Concrete in Compression," C512-82, American Society for Testing and Materials, Philadelphia, Pennsylvania.

7. CEB (European Concrete Committee), *International Recommendations for the Design and Construction of Concrete Structures, Principles and Recommendations*, Comité Européen du Béton, Paris, France, June 1970.

* * *